Published for SISSA by Springer

Received: November 26, 2024
Accepted: January 20, 2025
Published: February 19, 2025

Measurement of cross sections of $e^+e^- \to K^0_S K^0_S \psi(3686)$ from $\sqrt{s} = 4.682$ to 4.951 GeV

The BESIII collaboration

E-mail: BESIII-publications@ihep.ac.cn

Abstract: The process $e^+e^- \to K^0_S K^0_S \psi(3686)$ is studied by analyzing e^+e^- collision data samples collected at eight center-of-mass energies ranging from 4.682 to 4.951 GeV with the BESIII detector operating at the BEPCII collider, corresponding to an integrated luminosity of 4.1 fb^{-1}. Observation of the $e^+e^- \to K^0_S K^0_S \psi(3686)$ process is found for the first time with a statistical significance of 6.3σ, and the cross sections at each center-of-mass energy are measured. The ratio of cross sections of $e^+e^- \to K^0_S K^0_S \psi(3686)$ relative to $e^+e^- \to K^+K^- \psi(3686)$ is determined to be $\frac{\sigma(e^+e^- \to K^0_S K^0_S \psi(3686))}{\sigma(e^+e^- \to K^+K^- \psi(3686))} = 0.45 \pm 0.25$, which is consistent with the prediction based on isospin symmetry. The uncertainty includes both statistical and systematic contributions. Additionally, the $K^0_S \psi(3686)$ invariant mass distribution is found to be consistent with three-body phase space. The significance of a contribution beyond three-body phase space is only 0.8σ.

Keywords: e^+-e^- Experiments, Exotics

ArXiv ePrint: 2411.15752

https://doi.org/10.1007/JHEP02(2025)120

Contents

1 Introduction

Exotic hadrons, which are composed neither of a quark and anti-quark pair nor of three quarks, provide an unique opportunity to gain insight into the strong interaction. Since the discovery of the $\chi_{c1}(3872)$ state by the Belle experiment in 2003 [1], numerous unexpected charmonium-like states, including the $Y(4260)$ [2–4], $\psi(4660)$ [5–9], $Z_c(3900)$ [10, 11] and $Z_c(4020)$ [12], as well as the $Z_{cs}(3985)$ [13] and $Z_{cs}(4000)$ [14], have been observed by various experiments. The properties of these states do not match the predictions of conventional hadrons, and they are considered to be good candidates for exotic hadrons, such as hybrids [15–17], tetraquarks [18], meson molecules [19–21], hadro-charmonium [22, 23], or a combination thereof [24].

Several vector charmonium-like states have been reported based on a series of measurements of the cross sections of $e^+e^- \to$ hadrons, including both hidden-charm and open-charm processes [2, 4, 8, 25–32]. Three of these states, namely the $\psi(4660)$, $Y(4710)$, and $Y(4790)$, are located above 4.6 GeV. The $\psi(4660)$ resonance was first observed by the Belle Collaboration in $e^+e^- \to \pi^+\pi^-\psi(3686)$ via initial-state-radiation (ISR) [5], was subsequently confirmed by the BaBar [6] and BESIII [8] Collaborations in the same process, and was also seen in $e^+e^- \to \pi^+\pi^-\psi_2(3823)$ [9] by the BESIII Collaboration. Recently, BESIII measured the cross sections of $e^+e^- \to K\bar{K}J/\psi$ [33–36], leading to the discovery of the $Y(4710)$. Additionally, a structure around 4.79 GeV, referred to as the $Y(4790)$, was found to be essential to explain the cross section line-shape of $e^+e^- \to D_s^{*+}D_s^{*-}$ [37]. Potential models predict both the 5S and 4D charmonium states to be in this mass region [38–42]. Since the $Y(4710)$ and $Y(4790)$ are observed in final states containing $s\bar{s}c\bar{c}$ quark compositions, it is desirable to explore processes with similar quark compositions in the final state to uncover the nature of these vector structures.

In addition to the vector states, the BESIII experiment also observed the $Z_{cs}(3985)^+$ state, the strange partner of the Z_c states, in the process $e^+e^- \to K^\pm Z_{cs}(3985)^\mp$, $Z_{cs}(3985)^\pm \to (\bar{D}^0 D_s^{*\pm} + \bar{D}^{*0} D_s^\mp)$ [13]. Evidence of its neutral partner, the $Z_{cs}(3985)^0$, was also detected

JHEP02(2025)120

in the corresponding neutral process [43]. Meanwhile, the LHCb experiment observed two tetraquark candidates, the $Z_{cs}(4000)^+$ and $Z_{cs}(4220)^+$, decaying into K^+J/ψ in an amplitude analysis of $B^+ \to K^+\phi J/\psi$ [14]. There have been ongoing debates regarding whether the $Z_{cs}(3985)^+$ and $Z_{cs}(4000)^+$ are the same state, as they exhibit comparable masses but significantly different widths [44–52]. In the search for $Z_{cs}(3985)^\pm/Z_{cs}(4000)^\pm \to K^\pm J/\psi$ in $e^+e^- \to K^+K^-J/\psi$ by the BESIII experiment, no significant signal for the Z_{cs}^+ was found [53].

As an extension of the $e^+e^- \to K^+K^-J/\psi$ analysis, the $e^+e^- \to K^+K^-\psi(3686)$ process has also been investigated at BESIII using data samples taken at center-of-mass (c.m.) energies $\sqrt{s}$ ranging from 4.699 to 4.951 GeV [53]. The cross section line-shape shows an enhancement around 4.843 GeV, while no $Z_{cs}^\pm$ signal is seen.

In this analysis, the neutral process $e^+e^- \to K_S^0K_S^0\psi(3686)$ is studied using data samples collected at eight c.m. energies from 4.682 to 4.951 GeV in 2020 and 2021, corresponding to a total integrated luminosity of 4.1 fb^{-1}. The c.m. energies of the data samples are determined by selecting $e^+e^- \to \Lambda_c^+\bar{\Lambda}_c^-$ events [54], and the luminosities are measured using large-angle Bhabha events [54].

2 BESIII detector and data samples

The BESIII detector [55] records symmetric e^+e^- collisions provided by the BEPCII storage ring [56], which operates with a peak luminosity of $1.1 \times 10^{33}\,\mathrm{cm^{-2}s^{-1}}$ in the $\sqrt{s}$ range from 1.85 to 4.95 GeV [57]. The cylindrical core of the BESIII detector covers 93% of the full solid angle and consists of a helium-based multilayer drift chamber (MDC), a plastic scintillator time-of-flight system (TOF), and a CsI(Tl) electromagnetic calorimeter (EMC), which are all enclosed in a superconducting solenoidal magnet providing a 1.0 T magnetic field. The solenoid is supported by an octagonal flux-return yoke with resistive plate counter muon identification modules interleaved with steel. The charged-particle momentum resolution at 1 GeV/c is 0.5%, and the dE/dx resolution is 6% for electrons from Bhabha scattering. The EMC measures photon energies with a resolution of 2.5% (5%) at 1 GeV in the barrel (end-cap) region. The time resolution in the TOF barrel region is 68 ps, while that in the end-cap region is 110 ps. The end-cap TOF system was upgraded in 2015 using multi-gap resistive plate chamber technology, providing a time resolution of 60 ps, which benefits all of the data used in this analysis [58–60].

Monte Carlo (MC) samples are used to determine the detection efficiencies and to estimate the background contributions. MC samples are produced with a GEANT4-based [61] package, which includes the geometric description of the BESIII detector and the detector response. The simulation models the beam energy spread and initial state radiation in the e^+e^- annihilations with the generator KKMC [62, 63]. All particle decays are simulated by EVTGEN [64] with branching fractions either taken from the Particle Data Group (PDG) [65], when available, or otherwise estimated with LUNDCHARM [66]. Final state radiation from charged final state particles is incorporated using PHOTOS [67]. The inclusive MC samples include the production of open charm processes, the ISR production of vector charmonium(-like) states, and the continuum process incorporated in KKMC [62, 63].

In the MC simulation of the signal process, the $\psi(3686)$ decays to a J/ψ and other particles, including $\psi(3686) \to J/\psi + (\pi^+\pi^-, \pi^0\pi^0, \eta, \pi^0, \gamma\gamma)$, where $\gamma\gamma$ refers to the process

JHEP02(2025)120

$\psi(3686) \to \gamma\chi_{cJ}$, $\chi_{cJ} \to \gamma J/\psi$. The numbers of events generated for the different decay modes of the $\psi(3686)$ are normalized according to the corresponding branching fractions.

3 Event selection and background analysis

To identify candidate events of interest, each of the two K_S^0 is reconstructed using $K_S^0 \to \pi^+\pi^-$, the $\psi(3686)$ is reconstructed using $\psi(3686) \to J/\psi + X$, and the J/ψ using $J/\psi \to l^+l^-$ ($l = e, \mu$) decays. The particles accompanying the J/ψ in the $\psi(3686)$ decays, denoted by X, are not reconstructed in order to increase statistics. The following criteria are applied to select candidate events for the final state $\pi^+\pi^-\pi^+\pi^-l^+l^-X$.

A charged track must have a distance of closest approach to the interaction point (IP) less than 10 cm along the z axis ($|V_z| < 10.0\,\mathrm{cm}$) and less than 1 cm in the transverse plane ($|V_{xy}| < 1\,\mathrm{cm}$), and a polar angle ($\theta$) range of $|\cos\theta| < 0.93$. The z axis is the symmetry axis of the MDC, and θ is defined with respect to the z axis. In addition, the momentum of a lepton candidate (e or μ) is required to be greater than $1.2\,\mathrm{GeV}/c$. At least two leptons with opposite charge are required to be present in the candidate event.

To select charged pions from K_S^0 decays, the $|V_z|$ and $|V_{xy}|$ requirements are not applied. Assuming they are pions, a vertex fit is performed for each pair of charged tracks. To reject random $\pi^+\pi^-$ combinations, a secondary-vertex fit algorithm is employed to impose a kinematic constraint between the production and decay vertices [68]. The K_S^0 mass window is set to be $(0.490,\ 0.505)\,\mathrm{GeV}/c^2$. For each signal event candidate, there must be at least one $K_S^0K_S^0$ pair without overlapping pions. If there are two or more $K_S^0K_S^0$ pair candidates in the event, all combinations are kept for further study. The scatter plot of $M(\pi^+\pi^-)_1$ versus $M(\pi^+\pi^-)_2$ of the selected $K_S^0K_S^0$ pairs from all data samples combined is shown in figure 1(a).

A lepton candidate with more than 0.8 GeV of energy deposited in the calorimeter is assigned to be an electron, and a candidate depositing less than 0.5 GeV is assigned to be a muon [53]. To improve the efficiency, this requirement is also applied to just one of the two leptons. If both tracks satisfy this requirement, or if one track does not have EMC information and the other track satisfies this requirement, they are both retained. The invariant mass of the lepton pair $M(l^+l^-)$ is used to identify the J/ψ, within a mass window of $(3.05,\ 3.15)\,\mathrm{GeV}/c^2$, according to the mass resolution obtained from the simulation. The $M(l^+l^-)$ distributions from all data samples are shown in figures 1(b) and 1(c).

The fraction of events containing more than one combination is 8.9%, as estimated by the signal MC simulation at $\sqrt{s} = 4.843\,\mathrm{GeV}$, but it is 0 events in data. The fractions in other samples are at a similar level. The background contribution from multiple combinations in data is negligible. For events with multiple survived combinations in the signal MC simulation, the best one is identified using $\chi^2_{\mathrm{match}} = \sum_{i=1}^{4}(\mathbf{p}_i^{\mathrm{rec}} - \mathbf{p}_i^{\mathrm{truth}})^2$, where $\mathbf{p}_i^{\mathrm{rec}}$ is the 4-momenta of the reconstructed pion, and $\mathbf{p}_i^{\mathrm{truth}}$ is from the MC truth information. The $K_S^0K_S^0$ recoil mass spectrum ($M^{\mathrm{rec}}_{K_S^0K_S^0}$) from wrong combinations exhibits a flat distribution.

The inclusive MC sample is used to study remaining background contributions. The background is found to be negligible, and smoothly distributed in the $M^{\mathrm{rec}}_{K_S^0K_S^0}$ distribution, as shown in figure 2.

JHEP02(2025)120

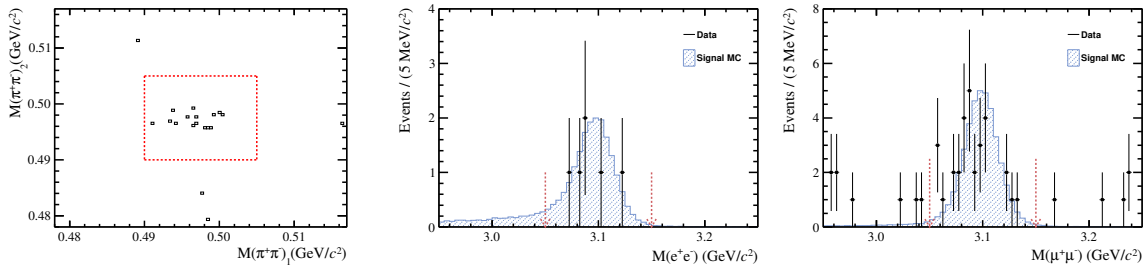

(a) (b) (c)

Figure 1. (a) The scatter plot of $M(\pi^+\pi^-)_1$ versus $M(\pi^+\pi^-)_2$ from the sum of all data, where the red square denotes the K^0_S signal region. (b) The $M(e^+e^-)$ and (c) the $M(\mu^+\mu^-)$ distribution obtained from the sum of all data, where the dots with error bars are data, the blue histograms are the sum of all signal MC samples at different energy points normalized according to the integrated luminosity, and the red dashed lines indicate the J/ψ mass window.

$\sqrt{s}$ (GeV)	$N_{\rm sdb}$	$N_{\rm obs}$	$N_{\rm sig}$	$N^{\rm C.I.}_{\rm sig}$	ϵ_{ee} (%)	$\epsilon_{\mu\mu}$ (%)	$(1+\delta)$	$\delta^{\rm VP}$	$\sigma_{\rm Born}$ (pb)	$\sigma^{\rm C.I.}_{\rm Born}$ (pb)	$\mathcal{S}$ (σ)
4.682	1	0	$-0.5^{+1.1}_{-0.4}$	(0.0, 2.0)	18.3	26.3	0.97	1.05	$-0.0^{+0.1}_{-0.0} \pm 0.00$	(0.0, 0.1)	-
4.699	0	0	0	(0.0, 2.0)	20.8	29.8	1.19	1.05	$0.0^{+0.2}_{-0.0} \pm 0.00$	(0.0, 0.3)	-
4.740	0	2	$2.0^{+2.6}_{-1.3}$	(0.5, 5.3)	21.9	31.3	0.86	1.05	$1.4^{+1.9}_{-0.9} \pm 0.10$	(0.4, 3.8)	1.2σ
4.750	1	4	$3.5^{+3.4}_{-2.0}$	(0.0, 8.0)	22.0	31.0	0.71	1.05	$1.4^{+1.3}_{-0.8} \pm 0.09$	(0.0, 3.1)	1.7σ
4.781	2	2	$1.0^{+2.9}_{-1.4}$	(0.0, 4.8)	21.5	30.6	0.86	1.06	$0.2^{+0.7}_{-0.4} \pm 0.01$	(0.0, 1.1)	0.2σ
4.843	2	6	$5.0^{+3.8}_{-2.5}$	(0.6, 10.5)	16.5	23.8	0.89	1.06	$1.4^{+1.1}_{-0.7} \pm 0.09$	(0.2, 3.0)	2.1σ
4.918	3	1	$-0.5^{+2.7}_{-1.2}$	(0.0, 3.7)	15.3	21.9	1.05	1.06	$-0.3^{+1.8}_{-0.8} \pm 0.02$	(0.0, 2.5)	-
4.951	0	0	0	(0.0, 2.0)	12.4	17.9	1.20	1.06	$0.0^{+1.0}_{-0.0} \pm 0.00$	(0.0, 1.8)	-

Table 1. The numerical results at each c.m. energy, where the c.m. energies ($\sqrt{s}$) are rounded to the nearest MeV, $N_{\rm sdb}$ is the number of events in the $\psi(3686)$ sideband region, $N_{\rm obs}$ is the number of events in the $\psi(3686)$ signal region, $N_{\rm sig}$ is the calculated signal yield in the $\psi(3686)$ signal region, ϵ is the detection efficiency for corresponding lepton pair, $(1+\delta)$ is the ISR correction factor, $\delta^{\rm VP}$ is the vacuum polarization factor, $\sigma_{\rm Born}$ is the Born cross section, $\sigma^{\rm C.I.}_{\rm Born}$ is the C.I. at the 90% confidence level after taking into account systematic uncertainty, and $\mathcal{S}$ is the statistical significance.

4 Cross section and confidence interval

Figures 2 and 3 show the $M^{\rm rec}_{K^0_S K^0_S}$ distributions for accepted candidates at each c.m. energy point individually and combined, respectively. The signal yield is obtained by counting events in the $\psi(3686)$ signal region $(3.66,\ 3.71)\,{\rm GeV}/c^2$. The number of background events in the signal region is estimated using the sideband region, defined as $(3.54,\ 3.64)\,{\rm GeV}/c^2$ when $\sqrt{s} < 4.77\,{\rm GeV}$ and $(3.59,\ 3.64) \cup (3.73,\ 3.78)\,{\rm GeV}/c^2$ when $\sqrt{s} > 4.77\,{\rm GeV}$. Therefore, the normalized ratio f of sideband to signal regions is 0.50. The number of expected background events $N_{\rm b}$ is estimated with $f \cdot N_{\rm sdb}$, where $N_{\rm sdb}$ is the events in the sideband region. The number of observed events $N_{\rm obs}$ consists of both the number of expected background events $N_{\rm b}$ and the number of signal events $N_{\rm sig}$ ($N_{\rm sig} = N_{\rm obs} - f \cdot N_{\rm sdb}$) and follows a Poisson distribution.

JHEP02(2025)120

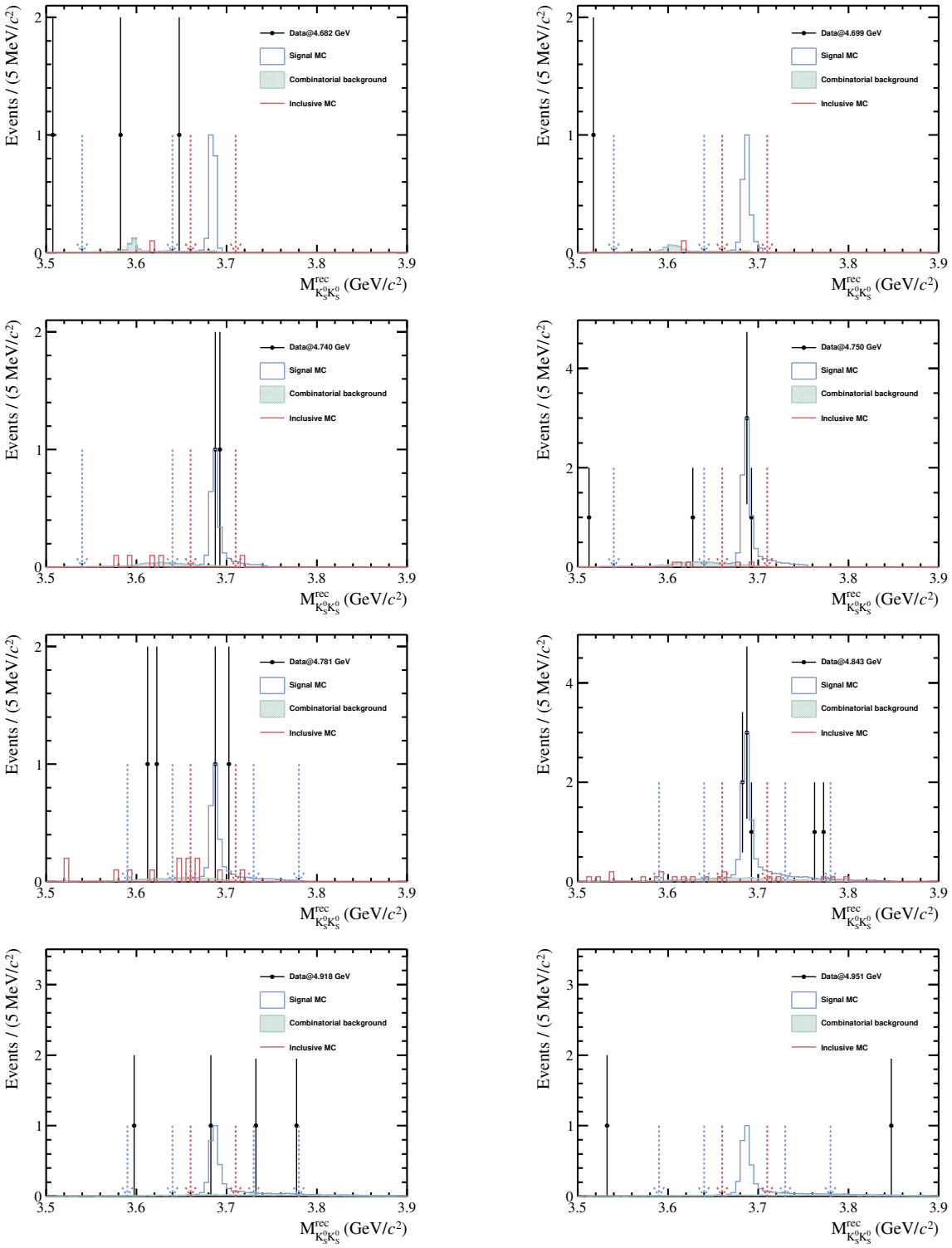

Figure 2. The $M^{\rm rec}_{K^0_SK^0_S}$ distributions for each c.m. energy. The black dots with error bars are data, and the red histograms are background contributions estimated by the inclusive MC sample, normalized according to the corresponding integrated luminosity. The blue histograms are the signal MC samples normalized according to the maximum number of events in any bin. The green histograms are the background from multiple combinations in the signal MC sample. The regions within the red and blue arrows indicate the $\psi(3686)$ signal and sideband regions, respectively.

JHEP02(2025)120

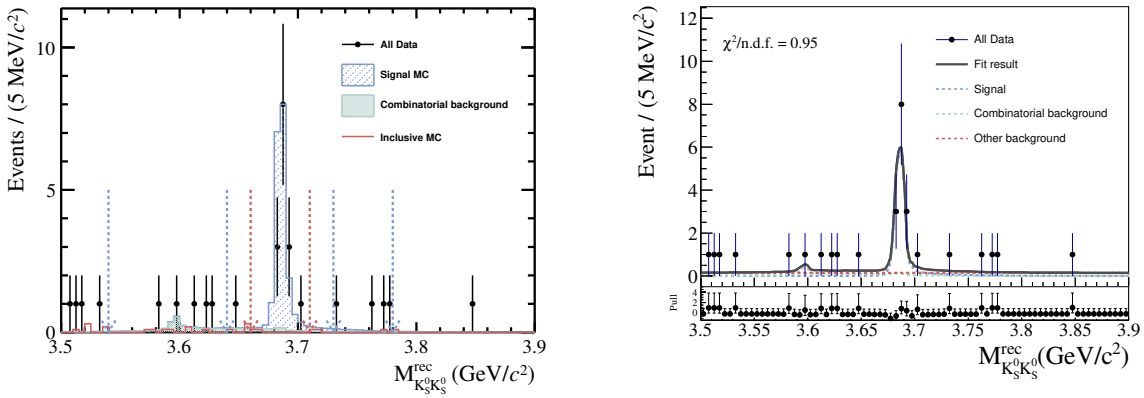

(a) (b)

Figure 3. (a) The $M^{\rm rec}_{K^0_S K^0_S}$ distributions from all c.m. energies combined. The black dots with error bars are data, and the red histograms are background contributions estimated by the inclusive MC sample, normalized according to the corresponding integrated luminosity. The blue histograms are the signal MC samples normalized according to integrated luminosity. The green histograms are the background from multiple combinations in the signal MC sample. The regions within the red and blue arrows indicate the $\psi(3686)$ signal and sideband regions, respectively. (b) The fit to the $M^{\rm rec}_{K^0_S K^0_S}$ distributions shown in (a). The black dots with error bars are data, and the solid black line represents the fitting result. The blue dashed curves are the signal components, the green dashed curves are the multi-combination background components, and the red dashed curves are the other background components.

The Born cross section $\sigma_{\rm Born}$, is calculated as:

$$\sigma_{\rm Born} = \frac{N_{\rm sig}}{\mathcal{L} \cdot \epsilon_r \cdot (1+\delta) \cdot \delta^{\rm VP}}, \tag{4.1}$$

where $\epsilon_r = \mathcal{B}^2(K^0_S \to \pi^+\pi^-) \cdot \mathcal{B}(\psi(3686) \to J/\psi X) \cdot \epsilon \cdot \mathcal{B}(J/\psi \to ll)$, $N_{\rm sig}$ is the number of $K^0_S K^0_S \psi(3686)$ signal events, $\mathcal{L}$ is the integrated luminosity, $\mathcal{B}$ is the branching fraction for each decay, ϵ is the detection efficiency obtained by subtracting the normalized efficiency in the sideband region from the efficiency in the signal region, $(1+\delta)$ is the ISR correction factor, and $\delta^{\rm VP}$ is the vacuum polarization factor taken from ref. [69]. Since there is no significant signal, the cross section line-shape from $e^+e^- \to K^+K^-\psi(3686)$ [53] is used for the calculation of the detection efficiency and ISR factor by the method described in ref. [70]. The obtained results are summarized in table 1.

The confidence interval (C.I.) of the cross section ($\sigma^{\rm C.I.}_{\rm Born}$) is determined by replacing $N_{\rm sig}$ with its C.I. $N^{\rm C.I.}_{\rm sig}$. The value of $N^{\rm C.I.}_{\rm sig}$ is determined by counting the number of events in the $\psi(3686)$ signal and sideband regions and using a frequentist method [71] with an unbounded profile likelihood. Assuming the signal and background yields follow a Poisson distribution and the detection efficiency follows a Gaussian distribution, TROLKE package [72] in the CERNROOT framework [73] is used to determine the C.I. of the cross section. The obtained results are also summarized in table 1.

The significance of the signal process at each c.m. energy is calculated by $\mathcal{P}$-value [74], $Z = \Phi^{-1}(1-\mathcal{P})$, where Z is the significance, and Φ^{-1} is the quantile of the normal

JHEP02(2025)120

distribution, assuming all observed events are background events and that $N_{\rm obs}$ follows a Poisson distribution. After considering the uncertainty on $N_{\rm b}$ [75], we use ROOSTATS package [76] in the CERNROOT framework [73] to obtain the statistical significance at each c.m. energy.

The significance of the signal process from all combined data samples is estimated by fitting to the total $M^{\rm rec}_{K^0_S K^0_S}$ distribution shown in figure 3(b). In the fit, signal events are described by the total signal MC shape, which is combined across different energy points by normalizing to the luminosity and detection efficiency. The multiple combinations are excluded from the signal MC shape by matching to the generated MC information. The contribution from multiple combinations in signal process is modeled using the corresponding MC shape, extracted from signal MC process with multiple combinations only. Other background contributions are described using a constant function. The signal yield and the number of other background events are free parameters, while the ratio of the number of multi-combinatorial background events and the number of signal events is fixed to that determined in the signal MC sample. The change in log likelihood values ($\Delta(-2\ln\mathcal{L})$), found by simultaneously removing the signal shape and the multi-combination background shape from the fit, is used to calculate the significance. The effects of the fitting range and background shape are considered, and in all cases, the statistical significance is above 6.0σ.

Figure 4(a) shows the Born cross section and the C.I. of $e^+e^- \to K^0_S K^0_S \psi(3686)$ at each c.m. energy. The ratio of $\sigma(e^+e^- \to K^0_S K^0_S \psi(3686))/\sigma(e^+e^- \to K^+K^-\psi(3686))$ is shown in figure 4(b), where the cross sections of $e^+e^- \to K^+K^-\psi(3686)$ are quoted from the measurements at BESIII [53]. The error bars shown in this figure include both statistical and systematic uncertainties of the cross section measurements. The common sources of systematic uncertainties, such as the luminosity, the ISR correction factor, and the J/ψ mass window, cancel between the two measurements. At energies 4.682, 4.699, and 4.740 GeV, the ratios are zero, and are not included in the fitting process. Fitting the ratios with a constant function leads to $\mathcal{R} = \sigma(e^+e^- \to K^0_S K^0_S \psi(3686))/\sigma(e^+e^- \to K^+K^-\psi(3686)) = 0.45 \pm 0.25$. The result is consistent with the expectation from isospin symmetry [77]. At 4.781, 4.843, and 4.918 GeV, the C.I. of the cross section ratios obtained by dividing the C.I. of $K^0_S K^0_S \psi(3686)$, by the cross section of $K^+K^-\psi(3686)$, are (0, 0.70), (0.10, 1.46), and (0, 2.36), respectively. These ratios include both statistical and systematic uncertainties, with the same systematic uncertainty canceling. The uncertainty of $K^+K^-\psi(3686)$ is taken into account when calculating the C.I. of $K^0_S K^0_S \psi(3686)$ using TROLKE package [72]. The results are shown in figure 4(b). The C.I. at 4.750 and 4.951 GeV are not included due to the large uncertainty of the cross section of $K^+K^-\psi(3686)$.

Intermediate states in the $K^0_S\psi(3686)$ system are investigated using data samples with $\sqrt{s}$ from 4.740 to 4.951 GeV. As each event contains two K^0_S mesons, we combine both K^0_S mesons with the $\psi(3686)$ for the invariant mass distribution of $K^0_S\psi(3686)$ (figure 5), resulting in each event appearing twice in the distribution. Assuming the observed events are all from $K^0_S K^0_S \psi(3686)$ three-body phase space, the $K^0_S\psi(3686)$ invariant mass distribution from MC simulation is displayed in the same figure. To evaluate the significance of possible contributions in addition to the $K^0_S K^0_S \psi(3686)$ three-body phase space, 20,000 sets of toy MC samples are produced using the sum of the phase space MC shape and the non-$\psi(3686)$

JHEP02(2025)120

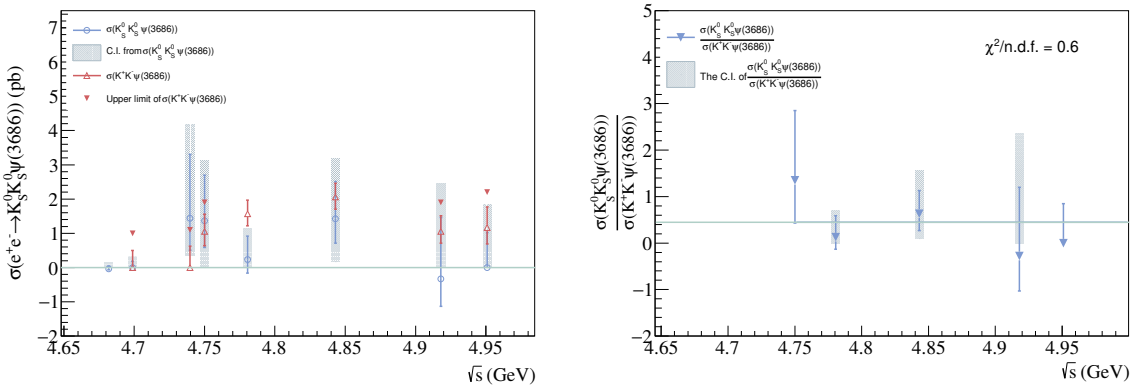

(a) (b)

Figure 4. (a) The Born cross section and C.I. of $\sigma(e^+e^- \to K^0_S K^0_S \psi(3686))$, where the blue dots with error bars are the measured Born cross sections, and the gray bands are the corresponding C.I. The Born cross section and the upper limit of the 90% confidence interval of $K^+K^-\psi(3686)$ are also shown in red, based on the published results [53]. The solid green line represents the cross section at 0. (b) The ratio $\frac{\sigma(e^+e^- \to K^0_S K^0_S \psi(3686))}{\sigma(e^+e^- \to K^+K^-\psi(3686))}$ at each data sample, where the gray bands are the corresponding C.I. The error bars include both statistical and systematic uncertainties, and the solid curve is the fit result.

events estimated from the sideband region in the data. In each toy MC sample, the number of entries is set to match the entries in data, as shown in figure 5(a). Fitting the toy MC samples with the same PDF as used in producing these samples, the $-\ln L$ distribution is shown in figure 5(b). The red vertical line indicates the $-\ln L$ value obtained from the fit to the data. The $\mathcal{P}$-value determined from the toy MC samples is 0.197, corresponding to a significance of 0.8σ for the deviation between the data and the model with the phase space contribution only.

5 Systematic uncertainty

The systematic uncertainties in the cross section measurement are caused by the luminosity, the tracking, the K^0_S reconstruction, the branching fraction, the kinematic fit, the ISR correction factor, the J/ψ mass window, and the $\psi(3686)$ signal and sideband regions. The systematic uncertainties are summarized in table 2 where the total systematic uncertainty is calculated as a sum in quadrature of all sources of uncertainty assuming they are independent.

The systematic uncertainties in the determination of the C.I. of the cross section can be classified as either additive or multiplicative terms. The additive terms include the $\psi(3686)$ signal and sideband region selections where these regions are varied, and the largest C.I. is chosen. The multiplicative systematic uncertainties are considered in the calculations of C.I.s by using the TROLKE package.

The integrated luminosity is measured by Bhabha events, with an uncertainty of 0.6% [54]. The systematic uncertainty from tracking is 1.0% per track [10]. The systematic uncertainty associated with K^0_S reconstruction is studied with the control sample $J/\psi \to K^*(892)^\pm K^\mp$ [78], and is assigned to be 1.2% per K^0_S. The uncertainties on the quoted branching fractions of different decays are taken from the PDG [65]. The helix parameters of the charged tracks are

JHEP02(2025)120

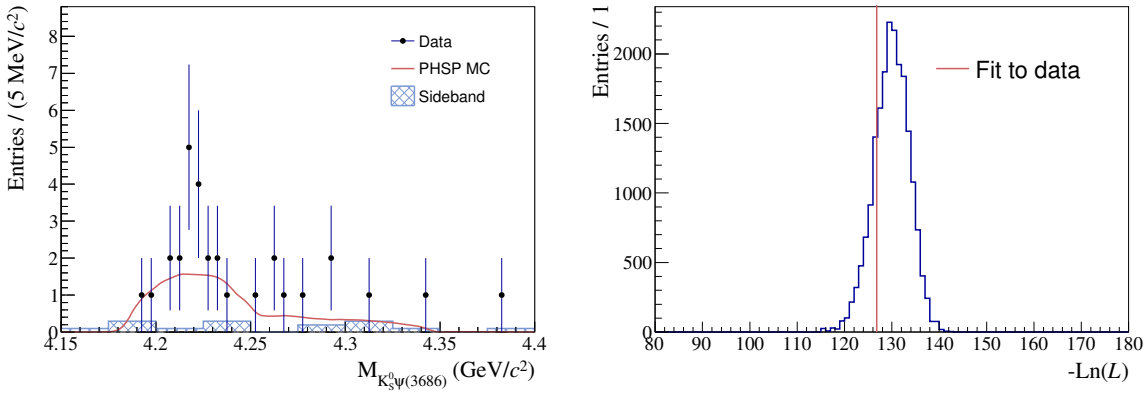

(a) (b)

Figure 5. (a) The $K^0_S\psi(3686)$ invariant mass distribution. The black dots with error bars are data in the $\psi(3686)$ signal region at $\sqrt{s}$ from 4.740 to 4.951 GeV, the blue histogram is the $\psi(3686)$ sideband region in data, and the red histogram is the $K^0_SK^0_S\psi(3686)$ three-body phase space MC sample at $\sqrt{s}$ from 4.740 to 4.951 GeV, normalized according to the cross sections. (b) The log-likelihood distribution obtained from fitting 20,000 sets of toy MC samples, where the blue histogram represents the log-likelihood distribution and the red vertical line indicates the log-likelihood value for the fit to the data.

corrected in simulation to improve the agreement of the χ^2 from the kinematic fit between data and MC simulation [79]. The systematic uncertainty from the kinematic fit is assigned as the difference in the efficiencies with and without this correction. The uncertainty from the ISR correction is estimated by sampling the parameters of the cross section line-shape $K^+K^-\psi(3686)$ 1000 times according to the covariance matrix given by the fit to the cross section [53]. The resultant distribution of $(1+\delta)\cdot\epsilon$ is fitted with a Gaussian function and the standard deviation is assigned as the systematic uncertainty. The 1.0% is accounted as a systematic uncertainty on the J/ψ mass window according to ref. [33].

In the cross section measurement, the systematic uncertainty due to the choices of $\psi(3686)$ signal and sideband regions are estimated by varying the boundaries of these sideband regions. To avoid the difference caused by statistical fluctuations, 1000 sets of toy MC samples are generated based on the fit results, then we fit the distribution of $M^{\rm rec}_{K^0_SK^0_S}$. In the fit, the signal is described by the MC shape, and the background is described by a first-order Chebyshev function. Then, $[(N/\epsilon)_{\rm nominal}-(N/\epsilon)_{\rm change}]/(N/\epsilon)_{\rm nominal}$ is calculated and modeled with a Gaussian function. The mean value of the Gaussian function represents the difference between the modified and nominal regions, and is taken as the corresponding uncertainty.

6 Summary

In summary, the $e^+e^-\to K^0_SK^0_S\psi(3686)$ process is studied using data samples accumulated at c.m. energies from 4.682 to 4.951 GeV with the BESIII detector at BEPCII. The cross sections of $e^+e^-\to K^0_SK^0_S\psi(3686)$ at different c.m. energy points are measured for the first time. The statistical significance of $e^+e^-\to K^0_SK^0_S\psi(3686)$ is 6.3σ when summing over all data samples. The C.I. at the 90% confidence level is provided for each data sample. In addition, the ratio

JHEP02(2025)120

Source/$\sqrt{s}$ (GeV)	4.682	4.699	4.740	4.750	4.781	4.843	4.918	4.951
Luminosity	0.6	0.6	0.6	0.6	0.6	0.6	0.6	0.6
Tracking	2.0	2.0	2.0	2.0	2.0	2.0	2.0	2.0
K_S^0 reconstruction	2.4	2.4	2.4	2.4	2.4	2.4	2.4	2.4
Branching fraction	1.1	1.1	1.1	1.1	1.1	1.1	1.1	1.1
Kinematic fit	0.2	0.3	0.3	0.3	0.2	0.2	0.2	0.2
ISR correction	1.0	1.2	3.0	1.5	0.6	0.2	0.6	0.5
J/ψ mass window	1.0	1.0	1.0	1.0	1.0	1.0	1.0	1.0
$\psi(3686)$ signal region*	2.8	2.8	2.8	2.8	2.8	2.8	2.8	2.8
$\psi(3686)$ sideband region*	4.8	4.8	4.8	4.8	4.8	4.8	4.8	4.8
Sum	6.7	6.7	7.2	6.7	7.3	6.6	6.6	6.6

Table 2. Relative systematic uncertainties (%) in the cross section measurement at each c.m. energy point, where the sources marked with * indicate additive uncertainties and the rest are multiplicative uncertainties.

$\sigma(e^+e^- \to K_S^0 K_S^0 \psi(3686))/\sigma(e^+e^- \to K^+K^-\psi(3686))$ is determined to be 0.45 ± 0.25, where the uncertainty includes both statistical and systematic uncertainties. The results agree with the predictions based on isospin symmetry within uncertainties. We search for the Z_{cs} state in the $Z_{cs} \to K_S^0\psi(3686)$ decay using data samples taken at $\sqrt{s} = 4.740 - 4.951\,\text{GeV}$. The $K_S^0\psi(3686)$ invariant mass distribution is consistent with three-body phase space, and no obvious structure is found. Larger data samples are needed to further investigate the vector states and the Z_{cs} in this process.

Acknowledgments

The BESIII Collaboration thanks the staff of BEPCII and the IHEP computing center for their strong support. This work is supported in part by National Key R&D Program of China under Contracts Nos. 2020YFA0406300, 2020YFA0406400, 2023YFA1606000; National Natural Science Foundation of China (NSFC) under Contracts Nos. 12375070, 11635010, 11735014, 11935015, 11935016, 11935018, 12025502, 12035009, 12035013, 12061131003, 12192260, 12192261, 12192262, 12192263, 12192264, 12192265, 12221005, 12225509, 12235017, 12361141819; the Chinese Academy of Sciences (CAS) Large-Scale Scientific Facility Program; the CAS Center for Excellence in Particle Physics (CCEPP); Joint Large-Scale Scientific Facility Funds of the NSFC and CAS under Contract No. U2032108, U1832207; Shanghai Leading Talent Program of Eastern Talent Plan under Contract No. JLH5913002; 100 Talents Program of CAS; The Institute of Nuclear and Particle Physics (INPAC) and Shanghai Key Laboratory for Particle Physics and Cosmology; German Research Foundation DFG under Contracts Nos. FOR5327, GRK 2149; Istituto Nazionale di Fisica Nucleare, Italy; Knut and Alice Wallenberg Foundation under Contracts Nos. 2021.0174, 2021.0299; Ministry of Development of Turkey under Contract No. DPT2006K-120470; National Research Foundation of Korea under Contract No. NRF-2022R1A2C1092335; National Science and

JHEP02(2025)120

Technology fund of Mongolia; National Science Research and Innovation Fund (NSRF) via the Program Management Unit for Human Resources & Institutional Development, Research and Innovation of Thailand under Contracts Nos. B16F640076, B50G670107; Polish National Science Centre under Contract No. 2019/35/O/ST2/02907; Swedish Research Council under Contract No. 2019.04595; The Swedish Foundation for International Cooperation in Research and Higher Education under Contract No. CH2018-7756; U. S. Department of Energy under Contract No. DE-FG02-05ER41374

Data Availability Statement. This article has no associated data or the data will not be deposited.

Code Availability Statement. This article has no associated code or the code will not be deposited.

References

[1] Belle collaboration, *Observation of a narrow charmonium-like state in exclusive $B^{\pm} \to K^{\pm}\pi^{+}\pi^{-}J/\psi$ decays*, *Phys. Rev. Lett.* **91** (2003) 262001 [hep-ex/0309032] [INSPIRE].

[2] BaBar collaboration, *Observation of a broad structure in the $\pi^{+}\pi^{-}J/\psi$ mass spectrum around 4.26-GeV/c^2*, *Phys. Rev. Lett.* **95** (2005) 142001 [hep-ex/0506081] [INSPIRE].

[3] CLEO collaboration, *Charmonium decays of Y(4260), $\psi(4160)$ and $\psi(4040)$*, *Phys. Rev. Lett.* **96** (2006) 162003 [hep-ex/0602034] [INSPIRE].

[4] Belle collaboration, *Measurement of $e^{+}e^{-} \to \pi^{+}\pi^{-}J/\psi$ cross-section via initial state radiation at Belle*, *Phys. Rev. Lett.* **99** (2007) 182004 [arXiv:0707.2541] [INSPIRE].

[5] Belle collaboration, *Observation of Two Resonant Structures in $e^{+}e^{-}$ to $\pi^{+}\pi^{-}\psi(2S)$ via Initial State Radiation at Belle*, *Phys. Rev. Lett.* **99** (2007) 142002 [arXiv:0707.3699] [INSPIRE].

[6] BaBar collaboration, *Study of the reaction $e^{+}e^{-} \to \psi(2S)\pi^{-}\pi^{-}$ via initial-state radiation at BaBar*, *Phys. Rev. D* **89** (2014) 111103 [arXiv:1211.6271] [INSPIRE].

[7] Belle collaboration, *Measurement of $e^{+}e^{-} \to \pi^{+}\pi^{-}\psi(2S)$ via Initial State Radiation at Belle*, *Phys. Rev. D* **91** (2015) 112007 [arXiv:1410.7641] [INSPIRE].

[8] BESIII collaboration, *Cross section measurement of $e^{+}e^{-} \to \pi^{+}\pi^{-}\psi(3686)$ from $\sqrt{S} = 4.0076$ to 4.6984 GeV*, *Phys. Rev. D* **104** (2021) 052012 [arXiv:2107.09210] [INSPIRE].

[9] BESIII collaboration, *Observation of Resonance Structures in $e^{+}e^{-} \to \pi^{+}\pi^{-}\psi_2(3823)$ and Mass Measurement of $\psi_2(3823)$*, *Phys. Rev. Lett.* **129** (2022) 102003 [arXiv:2203.05815] [INSPIRE].

[10] BESIII collaboration, *Observation of a Charged Charmoniumlike Structure in $e^{+}e^{-} \to \pi^{+}\pi^{-}J/\psi$ at $\sqrt{s} = 4.26$ GeV*, *Phys. Rev. Lett.* **110** (2013) 252001 [arXiv:1303.5949] [INSPIRE].

[11] Belle collaboration, *Study of $e^{+}e^{-} \to \pi^{+}\pi^{-}J/\psi$ and Observation of a Charged Charmoniumlike State at Belle*, *Phys. Rev. Lett.* **110** (2013) 252002 [*Erratum ibid.* **111** (2013) 019901] [arXiv:1304.0121] [INSPIRE].

JHEP02(2025)120

[12] BESIII collaboration, *Observation of a Charged Charmoniumlike Structure $Z_c(4020)$ and Search for the $Z_c(3900)$ in $e^+e^- \to \pi^+\pi^- h_c$*, *Phys. Rev. Lett.* **111** (2013) 242001 [arXiv:1309.1896] [INSPIRE].

[13] BESIII collaboration, *Observation of a Near-Threshold Structure in the K^+ Recoil-Mass Spectra in $e^+e^- \to K^+(D_s^- D^{*0} + D_s^{*-} D^0)$*, *Phys. Rev. Lett.* **126** (2021) 102001 [arXiv:2011.07855] [INSPIRE].

[14] LHCb collaboration, *Observation of New Resonances Decaying to $J/\psi K^+$ and $J/\psi\phi$*, *Phys. Rev. Lett.* **127** (2021) 082001 [arXiv:2103.01803] [INSPIRE].

[15] S.-L. Zhu, *The possible interpretations of Y(4260)*, *Phys. Lett. B* **625** (2005) 212 [hep-ph/0507025] [INSPIRE].

[16] F.E. Close and P.R. Page, *Gluonic charmonium resonances at BaBar and BELLE?*, *Phys. Lett. B* **628** (2005) 215 [hep-ph/0507199] [INSPIRE].

[17] E. Kou and O. Pene, *Suppressed decay into open charm for the Y(4260) being an hybrid*, *Phys. Lett. B* **631** (2005) 164 [hep-ph/0507119] [INSPIRE].

[18] L. Maiani, F. Piccinini, A.D. Polosa and V. Riquer, *The Z(4430) and a New Paradigm for Spin Interactions in Tetraquarks*, *Phys. Rev. D* **89** (2014) 114010 [arXiv:1405.1551] [INSPIRE].

[19] M. Cleven et al., *$Y(4260)$ as the first S-wave open charm vector molecular state?*, *Phys. Rev. D* **90** (2014) 074039 [arXiv:1310.2190] [INSPIRE].

[20] G.-J. Ding, *Are Y(4260) and $Z_2^+(4250)D_1D$ or D_0D^* Hadronic Molecules?*, *Phys. Rev. D* **79** (2009) 014001 [arXiv:0809.4818] [INSPIRE].

[21] Q. Wang, C. Hanhart and Q. Zhao, *Decoding the riddle of $Y(4260)$ and $Z_c(3900)$*, *Phys. Rev. Lett.* **111** (2013) 132003 [arXiv:1303.6355] [INSPIRE].

[22] S. Dubynskiy and M.B. Voloshin, *Hadro-Charmonium*, *Phys. Lett. B* **666** (2008) 344 [arXiv:0803.2224] [INSPIRE].

[23] X. Li and M.B. Voloshin, *$Y(4260)$ and $Y(4360)$ as mixed hadrocharmonium*, *Mod. Phys. Lett. A* **29** (2014) 1450060 [arXiv:1309.1681] [INSPIRE].

[24] D.-Y. Chen, X. Liu and T. Matsuki, *Interference effect as resonance killer of newly observed charmoniumlike states $Y(4320)$ and $Y(4390)$*, *Eur. Phys. J. C* **78** (2018) 136 [arXiv:1708.01954] [INSPIRE].

[25] BESIII collaboration, *Precise measurement of the $e^+e^- \to \pi^+\pi^- J/\psi$ cross section at center-of-mass energies from 3.77 to 4.60 GeV*, *Phys. Rev. Lett.* **118** (2017) 092001 [arXiv:1611.01317] [INSPIRE].

[26] BESIII collaboration, *Study of the resonance structures in the process $e^+e^- \to \pi^+\pi^- J/\psi$*, *Phys. Rev. D* **106** (2022) 072001 [arXiv:2206.08554] [INSPIRE].

[27] BESIII collaboration, *Evidence of Two Resonant Structures in $e^+e^- \to \pi^+\pi^- h_c$*, *Phys. Rev. Lett.* **118** (2017) 092002 [arXiv:1610.07044] [INSPIRE].

[28] BESIII collaboration, *Cross section measurements of $e^+e^- \to \omega\chi_{c0}$ form $\sqrt{s} = 4.178$ to 4.278 GeV*, *Phys. Rev. D* **99** (2019) 091103 [arXiv:1903.02359] [INSPIRE].

[29] BESIII collaboration, *Evidence of a resonant structure in the $e^+e^- \to \pi^+ D^0 D^{*-}$ cross section between 4.05 and 4.60 GeV*, *Phys. Rev. Lett.* **122** (2019) 102002 [arXiv:1808.02847] [INSPIRE].

[30] BESIII collaboration, *Observation of Three Charmoniumlike States with $J^{PC} = 1^{--}$ in $e^+e^- \to D^{*0}D^{*-}\pi^+$*, *Phys. Rev. Lett.* **130** (2023) 121901 [arXiv:2301.07321] [INSPIRE].

JHEP02(2025)120

[31] BESIII collaboration, *Observation of the $Y(4220)$ and $Y(4360)$ in the process $e^+e^- \to \eta J/\psi$*, *Phys. Rev. D* **102** (2020) 031101 [arXiv:2003.03705] [INSPIRE].

[32] BESIII collaboration, *Measurement of $e^+e^- \to \eta J/\psi$ cross section from $\sqrt{s} = 3.808$ GeV to 4.951 GeV*, *Phys. Rev. D* **109** (2024) 092012 [arXiv:2310.03361] [INSPIRE].

[33] BESIII collaboration, *Observation of the Y(4230) and evidence for a new vector charmoniumlike state Y(4710) in $e^+e^- \to K^0_S K^0_S J/\psi$*, *Phys. Rev. D* **107** (2023) 092005 [arXiv:2211.08561] [INSPIRE].

[34] BESIII collaboration, *Observation of $e^+e^- \to K\bar{K}J/\psi$ at center-of-mass energies from 4.189 to 4.600 GeV*, *Phys. Rev. D* **97** (2018) 071101 [arXiv:1802.01216] [INSPIRE].

[35] (BESIII) et al. collaborations, *Observation of the Y(4230) and a new structure in*, *Chin. Phys. C* **46** (2022) 111002 [arXiv:2204.07800] [INSPIRE].

[36] BESIII collaboration, *Observation of a Vector Charmoniumlike State at 4.7 GeV/c^2 and Search for Z_{cs} in $e^+e^- \to K^+K^-J/\psi$*, *Phys. Rev. Lett.* **131** (2023) 211902 [arXiv:2308.15362] [INSPIRE].

[37] BESIII collaboration, *Precise Measurement of the $e^+e^- \to D_s^{*+}D_s^{*-}$ Cross Sections at Center-of-Mass Energies from Threshold to 4.95 GeV*, *Phys. Rev. Lett.* **131** (2023) 151903 [arXiv:2305.10789] [INSPIRE].

[38] N. Akbar, *Decay Properties of Conventional and Hybrid Charmonium Mesons*, *J. Korean Phys. Soc.* **77** (2020) 17 [arXiv:2002.09566] [INSPIRE].

[39] R. Chaturvedi and A.K. Rai, *Charmonium spectroscopy motivated by general features of pNRQCD*, *Int. J. Theor. Phys.* **59** (2020) 3508 [arXiv:1910.06025] [INSPIRE].

[40] M.A. Sultan, N. Akbar, B. Masud and F. Akram, *Higher Hybrid Charmonia in an Extended Potential Model*, *Phys. Rev. D* **90** (2014) 054001 [arXiv:1403.6941] [INSPIRE].

[41] L.-C. Gui et al., *Strong decays of higher charmonium states into open-charm meson pairs*, *Phys. Rev. D* **98** (2018) 016010 [arXiv:1801.08791] [INSPIRE].

[42] S. Kanwal, F. Akram, B. Masud and E.S. Swanson, *Charmonium spectrum in an unquenched quark model*, *Eur. Phys. J. A* **58** (2022) 219 [arXiv:2211.08015] [INSPIRE].

[43] BESIII collaboration, *Evidence for a Neutral Near-Threshold Structure in the K^0_S recoil-mass spectra in $e^+e^- \to K^0_S D_s^+ D^{*-}$ and $e^+e^- \to K^0_S D_s^{*+} D^-$*, *Phys. Rev. Lett.* **129** (2022) 112003 [arXiv:2204.13703] [INSPIRE].

[44] L. Maiani, A.D. Polosa and V. Riquer, *The new resonances Zcs(3985) and Zcs(4003) (almost) fill two tetraquark nonets of broken SU(3)f*, *Sci. Bull.* **66** (2021) 1616 [arXiv:2103.08331] [INSPIRE].

[45] P.-P. Shi, F. Huang and W.-L. Wang, *Hidden charm tetraquark states in a diquark model*, *Phys. Rev. D* **103** (2021) 094038 [arXiv:2105.02397] [INSPIRE].

[46] J.F. Giron, R.F. Lebed and S.R. Martinez, *Spectrum of hidden-charm, open-strange exotics in the dynamical diquark model*, *Phys. Rev. D* **104** (2021) 054001 [arXiv:2106.05883] [INSPIRE].

[47] Q.-N. Wang, W. Chen and H.-X. Chen, *Exotic molecular states and tetraquark states with $J^P = 0^+, 1^+, 2^+$*, *Chin. Phys. C* **45** (2021) 093102 [arXiv:2011.10495] [INSPIRE].

[48] J.-B. Wang et al., *The low-lying hidden- and double-charm tetraquark states in a constituent quark model with instanton-induced interaction*, *Eur. Phys. J. C* **82** (2022) 721 [arXiv:2204.13320] [INSPIRE].

JHEP02(2025)120

[49] M. Karliner and J.L. Rosner, *Configuration mixing in strange tetraquarks Zcs*, *Phys. Rev. D* **104** (2021) 034033 [arXiv:2107.04915] [INSPIRE].

[50] S. Han and L.-Y. Xiao, *Aspects of Zcs(3985) and Zcs(4000)*, *Phys. Rev. D* **105** (2022) 054008 [arXiv:2203.00168] [INSPIRE].

[51] L. Meng, B. Wang, G.-J. Wang and S.-L. Zhu, *Implications of the Zcs(3985) and Zcs(4000) as two different states*, *Sci. Bull.* **66** (2021) 2065 [arXiv:2104.08469] [INSPIRE].

[52] Z.-G. Wang, *Decay widths of Z_{cs}(3985/4000) based on rigorous quark-hadron duality*, *Chin. Phys. C* **46** (2022) 103106 [arXiv:2205.03203] [INSPIRE].

[53] BESIII collaboration, *Measurement of the $e^+e^- \to K^+K^-\psi(2S)$ Cross Section at Center-of-Mass Energies from 4.699 to 4.951 GeV and Search for $Z_{cs}^{\pm}$ in the $Z_{cs}^{\pm} \to K^{\pm}\psi(2S)$ Decay*, arXiv:2407.20009 [INSPIRE].

[54] BESIII collaboration, *Luminosities and energies of e^+e^- collision data taken between $\sqrt{s} = 4.61$ GeV and 4.95 GeV at BESIII*, *Chin. Phys. C* **46** (2022) 113003 [arXiv:2205.04809] [INSPIRE].

[55] BESIII collaboration, *Design and Construction of the BESIII Detector*, *Nucl. Instrum. Meth. A* **614** (2010) 345 [arXiv:0911.4960] [INSPIRE].

[56] C. Yu et al., *BEPCII Performance and Beam Dynamics Studies on Luminosity*, in the proceedings of the *7th International Particle Accelerator Conference*, Busan, South Korea, May 08–13 (2016) [DOI:10.18429/JACoW-IPAC2016-TUYA01] [INSPIRE].

[57] BESIII collaboration, *Future Physics Programme of BESIII*, *Chin. Phys. C* **44** (2020) 040001 [arXiv:1912.05983] [INSPIRE].

[58] X. Li et al., *Study of MRPC technology for BESIII endcap-TOF upgrade*, *Radiat. Detect. Technol. Methods* **1** (2017) 13 [INSPIRE].

[59] Y.-X. Guo et al., *The study of time calibration for upgraded end cap TOF of BESIII*, *Radiat. Detect. Technol. Methods* **1** (2017) 15 [INSPIRE].

[60] P. Cao et al., *Design and construction of the new BESIII endcap Time-of-Flight system with MRPC Technology*, *Nucl. Instrum. Meth. A* **953** (2020) 163053 [INSPIRE].

[61] GEANT4 collaboration, *GEANT4 - A Simulation Toolkit*, *Nucl. Instrum. Meth. A* **506** (2003) 250 [INSPIRE].

[62] S. Jadach, B.F.L. Ward and Z. Was, *The Precision Monte Carlo event generator K K for two fermion final states in e^+e^- collisions*, *Comput. Phys. Commun.* **130** (2000) 260 [hep-ph/9912214] [INSPIRE].

[63] S. Jadach, B.F.L. Ward and Z. Was, *Coherent exclusive exponentiation for precision Monte Carlo calculations*, *Phys. Rev. D* **63** (2001) 113009 [hep-ph/0006359] [INSPIRE].

[64] D.J. Lange, *The EvtGen particle decay simulation package*, *Nucl. Instrum. Meth. A* **462** (2001) 152 [INSPIRE].

[65] Particle Data Group collaboration, *Review of Particle Physics*, *PTEP* **2022** (2022) 083C01 [INSPIRE].

[66] J.C. Chen et al., *Event generator for J/ψ and $\psi(2S)$ decay*, *Phys. Rev. D* **62** (2000) 034003 [INSPIRE].

[67] E. Richter-Was, *QED bremsstrahlung in semileptonic B and leptonic τ decays*, *Phys. Lett. B* **303** (1993) 163 [INSPIRE].

JHEP02(2025)120

[68] M. Xu et al., *Decay vertex reconstruction and 3-dimensional lifetime determination at BESIII*, *Chin. Phys. C* **33** (2009) 428 [INSPIRE].

[69] WORKING GROUP ON RADIATIVE CORRECTIONS and MONTE CARLO GENERATORS FOR LOW ENERGIES collaborations, *Quest for precision in hadronic cross sections at low energy: Monte Carlo tools vs. experimental data*, *Eur. Phys. J. C* **66** (2010) 585 [arXiv:0912.0749] [INSPIRE].

[70] W. Sun et al., *An iterative weighting method to apply ISR correction to e^+e^- hadronic cross-section measurements*, *Front. Phys. (Beijing)* **16** (2021) 64501 [arXiv:2011.07889] [INSPIRE].

[71] W.A. Rolke, A.M. Lopez and J. Conrad, *Limits and confidence intervals in the presence of nuisance parameters*, *Nucl. Instrum. Meth. A* **551** (2005) 493 [physics/0403059] [INSPIRE].

[72] *class TRolke: public TObject*, https://root.cern.ch/root/html604/TRolke.html.

[73] *ROOT Manual*, https://root.cern/manual/.

[74] G. Cowan, *Statistical data analysis*, Oxford University Press, Oxford (1998) [INSPIRE].

[75] R.D. Cousins, J.T. Linnemann and J. Tucker, *Evaluation of three methods for calculating statistical significance when incorporating a systematic uncertainty into a test of the background-only hypothesis for a Poisson process*, *Nucl. Instrum. Meth. A* **595** (2008) 480 [physics/0702156] [INSPIRE].

[76] *rs_numbercountingutils.C File Reference*, https://root.cern/doc/master/rs___numbercountingutils_8C.html.

[77] J.D. Bjorken and S.D. Drell, *Relativistic Quantum Mechanics*, McGraw-Hill, New York, U.S.A. (1965) [INSPIRE].

[78] BESIII collaboration, *Study of decay dynamics and CP asymmetry in $D^+ \to K^0_L e^+ \nu_e$ decay*, *Phys. Rev. D* **92** (2015) 112008 [arXiv:1510.00308] [INSPIRE].

[79] BESIII collaboration, *Search for hadronic transition $\chi_{cJ} \to \eta_c \pi^+ \pi^-$ and observation of $\chi_{cJ} \to K\overline{K}\pi\pi\pi$*, *Phys. Rev. D* **87** (2013) 012002 [arXiv:1208.4805] [INSPIRE].

JHEP02(2025)120

The BESIII collaboration

M. Ablikim[1], M.N. Achasov[4,c], P. Adlarson[76], O. Afedulidis[3], X.C. Ai[81], R. Aliberti[35], A. Amoroso[75A,75C], Q. An[72,58,a], Y. Bai[57], O. Bakina[36], I. Balossino[29A], Y. Ban[46,h], H.-R. Bao[64], V. Batozskaya[1,44], K. Begzsuren[32], N. Berger[35], M. Berlowski[44], M. Bertani[28A], D. Bettoni[29A], F. Bianchi[75A,75C], E. Bianco[75A,75C], A. Bortone[75A,75C], I. Boyko[36], R.A. Briere[5], A. Brueggemann[69], H. Cai[77], X. Cai[1,58], A. Calcaterra[28A], G.F. Cao[1,64], N. Cao[1,64], S.A. Cetin[62A], X.Y. Chai[46,h], J.F. Chang[1,58], G.R. Che[43], Y.Z. Che[1,58,64], G. Chelkov[36,b], C. Chen[43], C.H. Chen[9], Chao Chen[55], G. Chen[1], H.S. Chen[1,64], H.Y. Chen[20], M.L. Chen[1,58,64], S.J. Chen[42], S.L. Chen[45], S.M. Chen[61], T. Chen[1,64], X.R. Chen[31,64], X.T. Chen[1,64], Y.B. Chen[1,58], Y.Q. Chen[34], Z.J. Chen[25,i], S.K. Choi[10], G. Cibinetto[29A], F. Cossio[75C], J.J. Cui[50], H.L. Dai[1,58], J.P. Dai[79], A. Dbeyssi[18], R. E. de Boer[3], D. Dedovich[36], C.Q. Deng[73], Z.Y. Deng[1], A. Denig[35], I. Denysenko[36], M. Destefanis[75A,75C], F. De Mori[75A,75C], B. Ding[67,1], X.X. Ding[46,h], Y. Ding[34], Y. Ding[40], J. Dong[1,58], L.Y. Dong[1,64], M.Y. Dong[1,58,64], X. Dong[77], M.C. Du[1], S.X. Du[81], Y.Y. Duan[55], Z.H. Duan[42], P. Egorov[36,b], G.F. Fan[42], J.J. Fan[19], Y.H. Fan[45], J. Fang[1,58], J. Fang[59], S.S. Fang[1,64], W.X. Fang[1], Y.Q. Fang[1,58], R. Farinelli[29A], L. Fava[75B,75C], F. Feldbauer[3], G. Felici[28A], C.Q. Feng[72,58], J.H. Feng[59], Y.T. Feng[72,58], M. Fritsch[3], C.D. Fu[1], J.L. Fu[64], Y.W. Fu[1,64], H. Gao[64], X.B. Gao[41], Y.N. Gao[19], Y.N. Gao[46,h], Yang Gao[72,58], S. Garbolino[75C], I. Garzia[29A,29B], P.T. Ge[19], Z.W. Ge[42], C. Geng[59], E.M. Gersabeck[68], A. Gilman[70], K. Goetzen[13], L. Gong[40], W.X. Gong[1,58], W. Gradl[35], S. Gramigna[29A,29B], M. Greco[75A,75C], M.H. Gu[1,58], Y.T. Gu[15], C.Y. Guan[1,64], A.Q. Guo[31,64], L.B. Guo[41], M.J. Guo[50], R.P. Guo[49], Y.P. Guo[12,g], A. Guskov[36,b], J. Gutierrez[27], K.L. Han[64], T.T. Han[1], F. Hanisch[3], X.Q. Hao[19], F.A. Harris[66], K.K. He[55], K.L. He[1,64], F.H. Heinsius[3], C.H. Heinz[35], Y.K. Heng[1,58,64], C. Herold[60], T. Holtmann[3], P.C. Hong[34], G.Y. Hou[1,64], X.T. Hou[1,64], Y.R. Hou[64], Z.L. Hou[1], B.Y. Hu[59], H.M. Hu[1,64], J.F. Hu[56,j], Q.P. Hu[72,58], S.L. Hu[12,g], T. Hu[1,58,64], Y. Hu[1], G.S. Huang[72,58], K.X. Huang[59], L.Q. Huang[31,64], P. Huang[42], X.T. Huang[50], Y.P. Huang[1], Y.S. Huang[59], T. Hussain[74], F. Hölzken[3], N. Hüsken[35], N. in der Wiesche[69], J. Jackson[27], S. Janchiv[32], Q. Ji[1], Q.P. Ji[19], W. Ji[1,64], X.B. Ji[1,64], X.L. Ji[1,58], Y.Y. Ji[50], X.Q. Jia[50], Z.K. Jia[72,58], D. Jiang[1,64], H.B. Jiang[77], P.C. Jiang[46,h], S.S. Jiang[39], T.J. Jiang[16], X.S. Jiang[1,58,64], Y. Jiang[64], J.B. Jiao[50], J.K. Jiao[34], Z. Jiao[23], S. Jin[42], Y. Jin[67], M.Q. Jing[1,64], X.M. Jing[64], T. Johansson[76], S. Kabana[33], N. Kalantar-Nayestanaki[65], X.L. Kang[9], X.S. Kang[40], M. Kavatsyuk[65], B.C. Ke[81], V. Khachatryan[27], A. Khoukaz[69], R. Kiuchi[1], O.B. Kolcu[62A], B. Kopf[3], M. Kuessner[3], X. Kui[1,64], N. Kumar[26], A. Kupsc[44,76], W. Kühn[37], W.N. Lan[19], T.T. Lei[72,58], Z.H. Lei[72,58], M. Lellmann[35], T. Lenz[35], C. Li[47], C. Li[43], C.H. Li[39], Cheng Li[72,58], D.M. Li[81], F. Li[1,58], G. Li[1], H.B. Li[1,64], H.J. Li[19], H.N. Li[56,j], Hui Li[43], J.R. Li[61], J.S. Li[59], K. Li[1], K.L. Li[19], L.J. Li[1,64], Lei Li[48], M.H. Li[43], P.L. Li[64], P.R. Li[38,k,l], Q.M. Li[1,64], Q.X. Li[50], R. Li[17,31], T. Li[50], T.Y. Li[43], W.D. Li[1,64], W.G. Li[1,a], X. Li[1,64], X.H. Li[72,58], X.L. Li[50], X.Y. Li[1,8], X.Z. Li[59], Y. Li[19], Y.G. Li[46,h], Z.J. Li[59], Z.Y. Li[79], C. Liang[42], H. Liang[72,58], Y.F. Liang[54], Y.T. Liang[31,64], G.R. Liao[14], Y.P. Liao[1,64], J. Libby[26], A. Limphirat[60], C.C. Lin[55], C.X. Lin[64], D.X. Lin[31,64], T. Lin[1], B.J. Liu[1], B.X. Liu[77], C. Liu[34], C.X. Liu[1], F. Liu[1], F.H. Liu[53], Feng Liu[6], G.M. Liu[56,j], H. Liu[38,k,l], H.B. Liu[15], H.H. Liu[1], H.M. Liu[1,64], Huihui Liu[21], J.B. Liu[72,58], K. Liu[38,k,l], K.Y. Liu[40], Ke Liu[22], L. Liu[72,58], L.C. Liu[43], Lu Liu[43], M.H. Liu[12,g], P.L. Liu[1], Q. Liu[64], S.B. Liu[72,58], T. Liu[12,g], W.K. Liu[43], W.M. Liu[72,58], X. Liu[38,k,l], X. Liu[39], Y. Liu[38,k,l], Y. Liu[81], Y.B. Liu[43], Z.A. Liu[1,58,64], Z.D. Liu[9], Z.Q. Liu[50], X.C. Lou[1,58,64], F.X. Lu[59], H.J. Lu[23], J.G. Lu[1,58], Y. Lu[7], Y.P. Lu[1,58], Z.H. Lu[1,64], C.L. Luo[41], J.R. Luo[59], M.X. Luo[80], T. Luo[12,g], X.L. Luo[1,58], X.R. Lyu[64], Y.F. Lyu[43], F.C. Ma[40], H. Ma[79], H.L. Ma[1], J.L. Ma[1,64], L.L. Ma[50], L.R. Ma[67], Q.M. Ma[1], R.Q. Ma[1,64], R.Y. Ma[19], T. Ma[72,58],

JHEP02(2025)120

X.T. Ma[1,64], X.Y. Ma[1,58], Y.M. Ma[31], F.E. Maas[18], I. MacKay[70], M. Maggiora[75A,75C], S. Malde[70], Y.J. Mao[46,h], Z.P. Mao[1], S. Marcello[75A,75C], Y.H. Meng[64], Z.X. Meng[67], J.G. Messchendorp[13,65], G. Mezzadri[29A], H. Miao[1,64], T.J. Min[42], R.E. Mitchell[27], X.H. Mo[1,58,64], B. Moses[27], N. Yu. Muchnoi[4,c], J. Muskalla[35], Y. Nefedov[36], F. Nerling[18,e], L.S. Nie[20], I.B. Nikolaev[4,c], Z. Ning[1,58], S. Nisar[11,m], Q.L. Niu[38,k,l], W.D. Niu[55], Y. Niu [50], S.L. Olsen[10,64], Q. Ouyang[1,58,64], S. Pacetti[28B,28C], X. Pan[55], Y. Pan[57], A. Pathak[10], Y.P. Pei[72,58], M. Pelizaeus[3], H.P. Peng[72,58], Y.Y. Peng[38,k,l], K. Peters[13,e], J.L. Ping[41], R.G. Ping[1,64], S. Plura[35], V. Prasad[33], F.Z. Qi[1], H.R. Qi[61], M. Qi[42], S. Qian[1,58], W.B. Qian[64], C.F. Qiao[64], J.H. Qiao[19], J.J. Qin[73], L.Q. Qin[14], L.Y. Qin[72,58], X.P. Qin[12,g], X.S. Qin[50], Z.H. Qin[1,58], J.F. Qiu[1], Z.H. Qu[73], C.F. Redmer[35], K.J. Ren[39], A. Rivetti[75C], M. Rolo[75C], G. Rong[1,64], Ch. Rosner[18], M.Q. Ruan[1,58], S.N. Ruan[43], N. Salone[44], A. Sarantsev[36,d], Y. Schelhaas[35], K. Schoenning[76], M. Scodeggio[29A], K.Y. Shan[12,g], W. Shan[24], X.Y. Shan[72,58], Z.J. Shang[38,k,l], J.F. Shangguan[16], L.G. Shao[1,64], M. Shao[72,58], C.P. Shen[12,g], H.F. Shen[1,8], W.H. Shen[64], X.Y. Shen[1,64], B.A. Shi[64], H. Shi[72,58], J.L. Shi[12,g], J.Y. Shi[1], S.Y. Shi[73], X. Shi[1,58], J.J. Song[19], T.Z. Song[59], W.M. Song[34,1], Y. J. Song[12,g], Y.X. Song[46,h,n], S. Sosio[75A,75C], S. Spataro[75A,75C], F. Stieler[35], S. S Su[40], Y.J. Su[64], G.B. Sun[77], G.X. Sun[1], H. Sun[64], H.K. Sun[1], J.F. Sun[19], K. Sun[61], L. Sun[77], S.S. Sun[1,64], T. Sun[51,f], Y.J. Sun[72,58], Y.Z. Sun[1], Z.Q. Sun[1,64], Z.T. Sun[50], C.J. Tang[54], G.Y. Tang[1], J. Tang[59], M. Tang[72,58], Y.A. Tang[77], L.Y. Tao[73], M. Tat[70], J.X. Teng[72,58], V. Thoren[76], W.H. Tian[59], Y. Tian[31,64], Z.F. Tian[77], I. Uman[62B], Y. Wan[55], S.J. Wang[50], B. Wang[1], Bo Wang[72,58], C. Wang[19], D.Y. Wang[46,h], H.J. Wang[38,k,l], J.J. Wang[77], J.P. Wang [50], K. Wang[1,58], L.L. Wang[1], L.W. Wang[34], M. Wang[50], N.Y. Wang[64], S. Wang[38,k,l], S. Wang[12,g], T. Wang[12,g], T.J. Wang[43], W. Wang[59], W. Wang[73], W.P. Wang[35,58,72,o], X. Wang[46,h], X.F. Wang[38,k,l], X.J. Wang[39], X.L. Wang[12,g], X.N. Wang[1], Y. Wang[61], Y.D. Wang[45], Y.F. Wang[1,58,64], Y.H. Wang[38,k,l], Y.L. Wang[19], Y.N. Wang[45], Y.Q. Wang[1], Yaqian Wang[17], Yi Wang[61], Z. Wang[1,58], Z.L. Wang[73], Z.Y. Wang[1,64], D.H. Wei[14], F. Weidner[69], S.P. Wen[1], Y.R. Wen[39], U. Wiedner[3], G. Wilkinson[70], M. Wolke[76], L. Wollenberg[3], C. Wu[39], J.F. Wu[1,8], L.H. Wu[1], L.J. Wu[1,64], Lianjie Wu[19], X. Wu[12,g], X.H. Wu[34], Y.H. Wu[55], Y.J. Wu[31], Z. Wu[1,58], L. Xia[72,58], X.M. Xian[39], B.H. Xiang[1,64], T. Xiang[46,h], D. Xiao[38,k,l], G.Y. Xiao[42], H. Xiao[73], Y. L. Xiao[12,g], Z.J. Xiao[41], C. Xie[42], X.H. Xie[46,h], Y. Xie[50], Y.G. Xie[1,58], Y.H. Xie[6], Z.P. Xie[72,58], T.Y. Xing[1,64], C.F. Xu[1,64], C.J. Xu[59], G.F. Xu[1], M. Xu[72,58], Q.J. Xu[16], Q.N. Xu[30], W.L. Xu[67], X.P. Xu[55], Y. Xu[40], Y.C. Xu[78], Z.S. Xu[64], F. Yan[12,g], L. Yan[12,g], W.B. Yan[72,58], W.C. Yan[81], W.P. Yan[19], X.Q. Yan[1,64], H.J. Yang[51,f], H.L. Yang[34], H.X. Yang[1], J.H. Yang[42], R.J. Yang[19], T. Yang[1], Y. Yang[12,g], Y.F. Yang[43], Y.X. Yang[1,64], Y.Z. Yang[19], Z.W. Yang[38,k,l], Z.P. Yao[50], M. Ye[1,58], M.H. Ye[8], Junhao Yin[43], Z.Y. You[59], B.X. Yu[1,58,64], C.X. Yu[43], G. Yu[13], J.S. Yu[25,i], M.C. Yu[40], T. Yu[73], X.D. Yu[46,h], C.Z. Yuan[1,64], J. Yuan[34], J. Yuan[45], L. Yuan[2], S.C. Yuan[1,64], Y. Yuan[1,64], Z.Y. Yuan[59], C.X. Yue[39], Ying Yue[19], A.A. Zafar[74], F.R. Zeng[50], S.H. Zeng[63], X. Zeng[12,g], Y. Zeng[25,i], Y.J. Zeng[59], Y.J. Zeng[1,64], X.Y. Zhai[34], Y.C. Zhai[50], Y.H. Zhan[59], A.Q. Zhang[1,64], B.L. Zhang[1,64], B.X. Zhang[1], D.H. Zhang[43], G.Y. Zhang[19], H. Zhang[72,58], H. Zhang[81], H.C. Zhang[1,58,64], H.H. Zhang[59], H.Q. Zhang[1,58,64], H.R. Zhang[72,58], H.Y. Zhang[1,58], J. Zhang[59], J. Zhang[81], J.J. Zhang[52], J.L. Zhang[20], J.Q. Zhang[41], J.S. Zhang[12,g], J.W. Zhang[1,58,64], J.X. Zhang[38,k,l], J.Y. Zhang[1], J.Z. Zhang[1,64], Jianyu Zhang[64], L.M. Zhang[61], Lei Zhang[42], P. Zhang[1,64], Q. Zhang[19], Q.Y. Zhang[34], R.Y. Zhang[38,k,l], S.H. Zhang[1,64], Shulei Zhang[25,i], X.M. Zhang[1], X. Y Zhang[40], X.Y. Zhang[50], Y. Zhang[1], Y. Zhang[73], Y. T. Zhang[81], Y.H. Zhang[1,58], Y.M. Zhang[39], Yan Zhang[72,58], Z.D. Zhang[1], Z.H. Zhang[1], Z.L. Zhang[34], Z.X. Zhang[19], Z.Y. Zhang[43],

JHEP02(2025)120

Z.Y. Zhang[77], Z.Z. Zhang[45], Zh. Zh. Zhang[19], G. Zhao[1], J.Y. Zhao[1,64], J.Z. Zhao[1,58], L. Zhao[1], Lei Zhao[72,58], M.G. Zhao[43], N. Zhao[79], R.P. Zhao[64], S.J. Zhao[81], Y.B. Zhao[1,58], Y.X. Zhao[31,64], Z.G. Zhao[72,58], A. Zhemchugov[36,b], B. Zheng[73], B.M. Zheng[34], J.P. Zheng[1,58], W.J. Zheng[1,64], X.R. Zheng[19], Y.H. Zheng[64], B. Zhong[41], X. Zhong[59], H. Zhou[35,50,o], J.Y. Zhou[34], S. Zhou[6], X. Zhou[77], X.K. Zhou[6], X.R. Zhou[72,58], X.Y. Zhou[39], Y.Z. Zhou[12,g], Z.C. Zhou[20], A.N. Zhu[64], J. Zhu[43], K. Zhu[1], K.J. Zhu[1,58,64], K.S. Zhu[12,g], L. Zhu[34], L.X. Zhu[64], S.H. Zhu[71], T.J. Zhu[12,g], W.D. Zhu[41], W.J. Zhu[1], W.Z. Zhu[19], Y.C. Zhu[72,58], Z.A. Zhu[1,64], J.H. Zou[1], J. Zu[72,58]

[1] *Institute of High Energy Physics, Beijing 100049, People's Republic of China*
[2] *Beihang University, Beijing 100191, People's Republic of China*
[3] *Bochum Ruhr-University, D-44780 Bochum, Germany*
[4] *Budker Institute of Nuclear Physics SB RAS (BINP), Novosibirsk 630090, Russia*
[5] *Carnegie Mellon University, Pittsburgh, Pennsylvania 15213, U.S.A.*
[6] *Central China Normal University, Wuhan 430079, People's Republic of China*
[7] *Central South University, Changsha 410083, People's Republic of China*
[8] *China Center of Advanced Science and Technology, Beijing 100190, People's Republic of China*
[9] *China University of Geosciences, Wuhan 430074, People's Republic of China*
[10] *Chung-Ang University, Seoul, 06974, Republic of Korea*
[11] *COMSATS University Islamabad, Lahore Campus, Defence Road, Off Raiwind Road, 54000 Lahore, Pakistan*
[12] *Fudan University, Shanghai 200433, People's Republic of China*
[13] *GSI Helmholtzcentre for Heavy Ion Research GmbH, D-64291 Darmstadt, Germany*
[14] *Guangxi Normal University, Guilin 541004, People's Republic of China*
[15] *Guangxi University, Nanning 530004, People's Republic of China*
[16] *Hangzhou Normal University, Hangzhou 310036, People's Republic of China*
[17] *Hebei University, Baoding 071002, People's Republic of China*
[18] *Helmholtz Institute Mainz, Staudinger Weg 18, D-55099 Mainz, Germany*
[19] *Henan Normal University, Xinxiang 453007, People's Republic of China*
[20] *Henan University, Kaifeng 475004, People's Republic of China*
[21] *Henan University of Science and Technology, Luoyang 471003, People's Republic of China*
[22] *Henan University of Technology, Zhengzhou 450001, People's Republic of China*
[23] *Huangshan College, Huangshan 245000, People's Republic of China*
[24] *Hunan Normal University, Changsha 410081, People's Republic of China*
[25] *Hunan University, Changsha 410082, People's Republic of China*
[26] *Indian Institute of Technology Madras, Chennai 600036, India*
[27] *Indiana University, Bloomington, Indiana 47405, U.S.A.*
[28] *INFN Laboratori Nazionali di Frascati , (A)INFN Laboratori Nazionali di Frascati, I-00044, Frascati, Italy; (B)INFN Sezione di Perugia, I-06100, Perugia, Italy; (C)University of Perugia, I-06100, Perugia, Italy*
[29] *INFN Sezione di Ferrara, (A)INFN Sezione di Ferrara, I-44122, Ferrara, Italy; (B)University of Ferrara, I-44122, Ferrara, Italy*
[30] *Inner Mongolia University, Hohhot 010021, People's Republic of China*
[31] *Institute of Modern Physics, Lanzhou 730000, People's Republic of China*
[32] *Institute of Physics and Technology, Peace Avenue 54B, Ulaanbaatar 13330, Mongolia*
[33] *Instituto de Alta Investigación, Universidad de Tarapacá, Casilla 7D, Arica 1000000, Chile*
[34] *Jilin University, Changchun 130012, People's Republic of China*
[35] *Johannes Gutenberg University of Mainz, Johann-Joachim-Becher-Weg 45, D-55099 Mainz, Germany*
[36] *Joint Institute for Nuclear Research, 141980 Dubna, Moscow region, Russia*
[37] *Justus-Liebig-Universitaet Giessen, II. Physikalisches Institut, Heinrich-Buff-Ring 16, D-35392 Giessen, Germany*
[38] *Lanzhou University, Lanzhou 730000, People's Republic of China*
[39] *Liaoning Normal University, Dalian 116029, People's Republic of China*

JHEP02(2025)120

[40] Liaoning University, Shenyang 110036, People's Republic of China
[41] Nanjing Normal University, Nanjing 210023, People's Republic of China
[42] Nanjing University, Nanjing 210093, People's Republic of China
[43] Nankai University, Tianjin 300071, People's Republic of China
[44] National Centre for Nuclear Research, Warsaw 02-093, Poland
[45] North China Electric Power University, Beijing 102206, People's Republic of China
[46] Peking University, Beijing 100871, People's Republic of China
[47] Qufu Normal University, Qufu 273165, People's Republic of China
[48] Renmin University of China, Beijing 100872, People's Republic of China
[49] Shandong Normal University, Jinan 250014, People's Republic of China
[50] Shandong University, Jinan 250100, People's Republic of China
[51] Shanghai Jiao Tong University, Shanghai 200240, People's Republic of China
[52] Shanxi Normal University, Linfen 041004, People's Republic of China
[53] Shanxi University, Taiyuan 030006, People's Republic of China
[54] Sichuan University, Chengdu 610064, People's Republic of China
[55] Soochow University, Suzhou 215006, People's Republic of China
[56] South China Normal University, Guangzhou 510006, People's Republic of China
[57] Southeast University, Nanjing 211100, People's Republic of China
[58] State Key Laboratory of Particle Detection and Electronics, Beijing 100049, Hefei 230026, People's Republic of China
[59] Sun Yat-Sen University, Guangzhou 510275, People's Republic of China
[60] Suranaree University of Technology, University Avenue 111, Nakhon Ratchasima 30000, Thailand
[61] Tsinghua University, Beijing 100084, People's Republic of China
[62] Turkish Accelerator Center Particle Factory Group, (A)Istinye University, 34010, Istanbul, Turkey; (B)Near East University, Nicosia, North Cyprus, 99138, Mersin 10, Turkey
[63] University of Bristol, H H Wills Physics Laboratory, Tyndall Avenue, Bristol, BS8 1TL, U.K.
[64] University of Chinese Academy of Sciences, Beijing 100049, People's Republic of China
[65] University of Groningen, NL-9747 AA Groningen, The Netherlands
[66] University of Hawaii, Honolulu, Hawaii 96822, U.S.A.
[67] University of Jinan, Jinan 250022, People's Republic of China
[68] University of Manchester, Oxford Road, Manchester, M13 9PL, United Kingdom
[69] University of Muenster, Wilhelm-Klemm-Strasse 9, 48149 Muenster, Germany
[70] University of Oxford, Keble Road, Oxford OX13RH, United Kingdom
[71] University of Science and Technology Liaoning, Anshan 114051, People's Republic of China
[72] University of Science and Technology of China, Hefei 230026, People's Republic of China
[73] University of South China, Hengyang 421001, People's Republic of China
[74] University of the Punjab, Lahore-54590, Pakistan
[75] University of Turin and INFN, (A)University of Turin, I-10125, Turin, Italy; (B)University of Eastern Piedmont, I-15121, Alessandria, Italy; (C)INFN, I-10125, Turin, Italy
[76] Uppsala University, Box 516, SE-75120 Uppsala, Sweden
[77] Wuhan University, Wuhan 430072, People's Republic of China
[78] Yantai University, Yantai 264005, People's Republic of China
[79] Yunnan University, Kunming 650500, People's Republic of China
[80] Zhejiang University, Hangzhou 310027, People's Republic of China
[81] Zhengzhou University, Zhengzhou 450001, People's Republic of China

[a] Deceased
[b] Also at the Moscow Institute of Physics and Technology, Moscow 141700, Russia
[c] Also at the Novosibirsk State University, Novosibirsk, 630090, Russia
[d] Also at the NRC "Kurchatov Institute", PNPI, 188300, Gatchina, Russia
[e] Also at Goethe University Frankfurt, 60323 Frankfurt am Main, Germany
[f] Also at Key Laboratory for Particle Physics, Astrophysics and Cosmology, Ministry of Education; Shanghai Key Laboratory for Particle Physics and Cosmology; Institute of Nuclear and Particle Physics, Shanghai 200240, People's Republic of China

JHEP02(2025)120

[g] Also at Key Laboratory of Nuclear Physics and Ion-beam Application (MOE) and Institute of Modern Physics, Fudan University, Shanghai 200443, People's Republic of China
[h] Also at State Key Laboratory of Nuclear Physics and Technology, Peking University, Beijing 100871, People's Republic of China
[i] Also at School of Physics and Electronics, Hunan University, Changsha 410082, China
[j] Also at Guangdong Provincial Key Laboratory of Nuclear Science, Institute of Quantum Matter, South China Normal University, Guangzhou 510006, China
[k] Also at MOE Frontiers Science Center for Rare Isotopes, Lanzhou University, Lanzhou 730000, People's Republic of China
[l] Also at Lanzhou Center for Theoretical Physics, Lanzhou University, Lanzhou 730000, People's Republic of China
[m] Also at the Department of Mathematical Sciences, IBA, Karachi 75270, Pakistan
[n] Also at Ecole Polytechnique Federale de Lausanne (EPFL), CH-1015 Lausanne, Switzerland
[o] Also at Helmholtz Institute Mainz, Staudinger Weg 18, D-55099 Mainz, Germany

JHEP02(2025)120